46th AIAA/ASME/SAE/ASEE Joint Propulsion Conference & Exhibit
25 - 28 July 2010, Nashville, TN

AIAA 2010-6940

Optimal Frequency for Plasma Heating with a Single Electrostatic Wave

Benjamin Jorns* and Edgar Y. Choueiri †
Electric Propulsion and Plasma Dynamics Laboratory
Princeton University, Princeton, NJ, 08544, USA

An experimental investigation of plasma heating by a single electrostatic wave (SEW) in a magnetized, rf-sustained plasma was carried out to establish the existence of an optimal wave frequency for maximized heating, which we recently predicted theoretically. A variable tuning network was constructed for electrostatic ion cyclotron wave launching, and laser-induced fluorescence measurements were made of ion heating and its dependence on SEW frequency over the tunable range of the second to the sixth harmonic of the ion cyclotron frequency. The measurements revealed a dependence of heating on frequency as predicted by the theory and the existence of an optimal frequency that is within one cyclotron harmonic from the theoretically predicted value. The findings establish a fundamental prescription for optimizing plasma heating by electrostatic waves, that is particularly useful for plasma propulsion where efficiency is of prime importance.

Nomenclature

ω	wave frequency
ν	wave frequency normalized by cyclotron frequency
k	wave number
E	wave amplitude
q	ion charge
ω_{ci}	ion cyclotron frequency
T_e	electron temperature
T_i	ion temperature
T_{i0}	background ion temperature
I	normalized kinetic energy
$v_\perp$	perpendicular ion velocity
m	mass of Ar ion

I. Introduction

The relative ease of implementing the radio frequency (RF) heating of plasma as well as its potential for high efficiency make this process an essential component for a number of industrial and scientific applications, and in recent years, these qualities have led to its incorporation as an effective heating element for electrothermal plasma propulsion. There are a number of methods for achieving the RF heating of a plasma,[1] but one that has enjoyed particular success relies on the non-linear interaction with ions of a single electrostatic wave (SEW) that propagates perpendicularly to the field of a uniformly magnetized plasma. This process was first explored analytically by Karney in 1977[2,3] who showed that significant ion acceleration can occur when the SEW is provided by a lower hybrid wave. Further work has explored the physical

*Graduate Research Assistant, EPPDyL
†Chief Scientist, EPPDyL; Professor, Applied Physics Group, Mechanical and Aerospace Engineering Department; Fellow AIAA.

implementation of this process in a plasma and found significant and efficient heating (a review of these experimental results can be found in Ref. 1 as well as Ref. 4). The process consequently has been employed in fusion experiments as well as been adapted with great success as a source for current drive in toroidal configuration plasmas.[5]

In a recent work,[6] we used second-order Lie transform theory to derive an expression for the frequency dependence of heating for a collisionless, test-particle collection of Maxwellian ions subject to SEW heating and an even more promising method that relies on beating electrostatic waves (BEW), which is described in Refs. 7–10. We found theoretically that there is an optimal frequency for each of the two mechanisms at which the greatest heating is produced. While this is a particularly exciting prospect for applications such as electrothermal plasma propulsion where efficiency of plasma heating is paramount, there is as of yet no experimental confirmation of these theoretical results.

The goal of this investigation then is to experimentally characterize the frequency dependence of the SEW process, establish the existence of an optimal frequency, and compare it to our previously derived predictions. This will be followed by a similar study in the near future for the case of BEW heating, which requires a more powerful rf amplifier than that we had for the present study.

To this end, this paper is structured in the following way. Section II provides a brief review of the theoretical background for plasma heating with SEW. Section III provides a description of the experimental setup as well as the experimental parameters. Section IV describes the dispersion relation and power for the waves used for this work. Sec V presents the frequency dependence of ion heating results. And finally, in Sec. VI we discuss the implications of the heating results in the context of theoretical work as well as future investigations.

II. Theoretical Background

We provide here a brief review of the derivations performed in Ref. 6 to find an approximation for the heating of a Maxwellian ion ensemble subject to SEW ion acceleration. In particular, by treating the ions as test-particles such that their dynamics do not affect wave propagation and by assuming the ensemble to be collisionless, we can find the heating of the ensemble simply by calculating the average increase in kinetic energy of the individual ions. This is done by first considering the normalized Hamiltonian governing single ion dynamics:

$$H = I + \varepsilon \cos(\sqrt{2I}\sin\theta - \nu\tau + \phi), \tag{1}$$

where $\tau = \omega_{ci}t$ is normalized time and $\varepsilon = (kqE)/(m\omega_{ci}^2)$ is the normalized wave amplitude. Here E is the electric field amplitude of the waves; q and m are the charge and mass of the ion respectively; k is the wavenumber of both waves; $I = (r_L k)^2/2$ is the action coordinate that scales with ion kinetic energy; r_L is the unperturbed Larmor radius of the ions; φ is the phase of the wave relative to the cyclotron motion; and θ is the cyclotron angle measured from the $\vec{B}\times\vec{k}$ direction. Without loss of generality, we let $\phi = 0$.

In order to describe the initial state of the ions, we use a density distribution isotropic in Larmor angle with a velocity distribution given by a two-dimensional, magnetized Maxwellian expressed in action-angle coordinates as $f(I_0) = \mu^{-1}e^{-I_0/\mu}$ where we have adopted the notation of Stix[11] so that $\mu = \frac{1}{2}k^2\langle r_L^2\rangle = \frac{1}{2}k^2\langle v_\perp^2\rangle/\omega_c^2 = k^2T_i/(m\omega_c^2)$; $\langle v_\perp\rangle = (T_{i0}/m)^{1/2}$ is the average (i.e. thermal) ion velocity perpendicular to the magnetic field, and T_{i0} is the temperature of the initial ion distribution. Physically, μ represents the extent of ion magnetization on the length scale of the wavelength. With this normalized Maxwellian and Eq. 1 describing individual ion dynamics, we now invoke our collisionless and test particle assumptions to find an expression for the average, normalized kinetic energy:

$$\langle I(\tau)\rangle = \int_0^\infty \langle I(I_0,\theta_0,\tau)\rangle_{\theta_0} f(I_0)dI_0, \tag{2}$$

where the integration is over the initial action and $\langle..\rangle_{\theta_0}$ is the average over initial Larmor angle. The non-linearity of Eq. 1 precludes a closed form solution for $I(I_0,\theta_0,\tau)$ and subsequent evaluation of Eq. 2. Therefore, in Ref. 6 we invoked phase-averaged, Lie transform theory to find a second-order expression for the averaged, normalized kinetic energy when it has equilibrated to a steady-state value:

$$\langle I_{eq}\rangle = \mu + \left(\frac{\varepsilon}{\|\nu\| - \nu}\right)^2 \frac{e^{-\mu}}{2\mu}\|\nu\|^2 I_{\|\nu\|}(\mu) \tag{3}$$

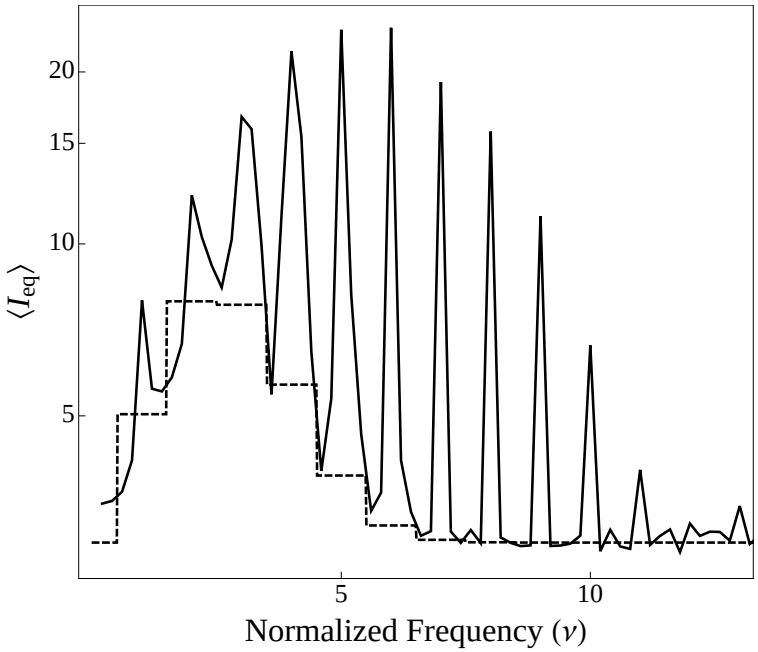

Figure 1. Plot of the analytically calculated envelope $h(\nu)$ (dotted line) as well as numerical results (solid line) for $\mu = 3$. These results are taken from Ref. 6

where $\|..\|$ denotes the nearest integer function and $I_{\|\nu_i\|}(\mu)$ is the modified Bessel function of the first kind. While μ is a constant that represents the initial average energy or background ion temperature, the other term depends on a number of wave and plasma parameters that dictate the degree of heating over background. The wave amplitude dependence is apparent in so much as to second-order, the heating scales with ε^2. However, we also see two additional, interesting trends from the second term of Eq. 3: improved heating near on-resonance and an optimal frequency for heating. We discuss each in turn using Figure 1 to illustrate the respective trends. The solid line in this graph represents the numerical results from Ref. 6 for SEW heating of a Maxwellian ion ensemble with initial parameter $\mu = 3$.

A. Improved heating at on-resonance

The factor $(\|\nu\| - \nu)^{-2}$ from Eq. 3 indicates that the proximity to the on-resonance condition ($\nu = n$ where n is an integer) directly impacts the level of heating. This is seen in the numerical results of Figure 1 where there is significantly improved heating at on-resonance.

B. Optimal frequency

The second term of Eq. 3, which we denote $h(\nu)$, also influences ion heating. A simplified approximation for this expression is given by

$$h(\nu) \approx \frac{1}{\sqrt{16\pi\mu^3}} \left[\|\nu\|^2 e^{-\frac{\|\nu\|^2}{2\mu}} \right]. \tag{4}$$

When plotted versus ν (dotted line in Figure 1), this term describes a convex envelope which exhibits a range of frequencies, denoted ν^*, that maximizes $h(\nu)$. The reason for this maximum is due to the fact that while the overall energy achieved by accelerated ions increases with frequency, the number of ions subject to acceleration *decreases* with higher frequencies. This results directly from the fact that SEW is a resonant process that can only target ions with initial perpendicular velocity $v_\perp$ that is comparable to the wave phase velocity: $v_\perp \sim \omega/k$ which in normalized coordinates is $\sqrt{2I} \sim \nu$. With this in mind, in Ref. 6 we found an approximation for the optimal range of frequencies for $h(\nu)$:

$$\|\nu^*\| = \sqrt{2I}. \tag{5}$$

Of course, this expression only serves as a rough indication of the optimal frequency for the *overall* heating, since as can be seen from Figure 1, the optimum of the envelope $h(\nu)$ does not correspond to the overall maximum, denoted $\overline{\nu}$. This is in part because the on-resonance effects skew the heating toward this differnent value, $\overline{\nu}$–although we do note that our numerical investigation revealed a similar scaling for this true, optimal frequency: $\overline{\nu} \propto \sqrt{\nu}$. This result is further complicated by the fact that we performed the above derivations with the generalizing assumption that the exciting waves were dispersionless, i.e. k is a constant such that μ is a constant. This is not necessarily the case in experimental applications, which is a point we address later.

Regardless, our numerical and analytical work has illustrated two important trends for ion heating and thus represents a benchmark for our experimental investigation. In the next section, we outline the setup of our experiment that explores this dependency.

III. Experimental Setup

For this experimental investigation, we employed an axially symmetric, uniformly magnetized plasma sustained by an inductive, RF discharge. The magnetic field used for our heating measures was 500 G ($f_{ci} \approx 19$ kHz) while the plasma source was operated at 250 W with a fill pressure of argon measured at 1 mT. This yielded an ion density of 10^{10} cm^{-3} and an electron temperature of approximately $T_e \approx 3$ eV. These experimental parameters were chosen for the investigation as we observed the highest levels of ion heating at these values. A more detailed description of these parameters is provided in Refs. 12 and 13 along with a full characterization of the experimental setup shown in Fig. 2. We provide here a brief overview of the different elements in the setup.

A. Vacuum Chamber and Solenoid

We employ a Pyrex cylinder 52" in length with a 6.5" inner diameter placed concentrically in a 48" long, 10 ring solenoid. A small window at the end of the chamber provides longitudinal optical access while argon gas flows into the chamber through a feed in the cross at the opposite end of the chamber. A constant pressure of 0.1 to 10 mTorr is maintained by a 140 l/s turbo pump with a conductance controller as well as a roughing pump.

Two klystron Varian 1955A magnets placed end to end provide a magnetic field in the experimental test region. Each magnet has been calibrated experimentally as well as numerically modeled to produce a uniform magnetic field in the experimental region with a magnitude of 500 $\pm$2.5 G. The plasma discharge propagates along the magnetic field lines generated by the solenoid into the uniform-field experimental region.

B. Plasma source

The plasma discharge is produced by a Boswell-type saddle antenna with a 7.25" inner diameter placed around the vacuum chamber at one end of the solenoid. The antenna is powered by a 1.25 kW source operated at 13.56 MHz and matched to the plasma with an L network consisting of two Jennings 1000 pF 3kV variable vacuum capacitors. In order to minimize RF noise from this antenna as well as provide a low energy background for contrast to the heating, we operated this antenna in the inductive mode at 250W.

C. Heating Antenna

We show an image of the heating antenna along with a schematic for its power supply and matching network in Fig. 2 . The antenna consists of a transverse Helmholtz configuration that is modeled after the successful rectangular antenna geometry employed by Kline for single electrostatic wave heating.[14] It is a 6" $\times$ 9" rectangle and consists of 40 loops on each coil mounted directly on the pyrex vacuum vessel. The coils are operated in phase from 2kHz to 20 MHz and powered with an ENI 100 W amplifier that is driven by one or two Wavetek 120 function generators. The second generator is for future two-wave heating experiments.

Since the electrostatic waves in the plasma are generated by the inductive excitation of the parallel component of the electrostatic ion cyclotron wave, the wave amplitude is heavily dependent on the magnetic flux generated by the coils and therefore the current generated in them. It is therefore desirable and necessary to employ an impedance matching network to maximize this current. To this end, we use a tuning network that consists of three parallel vacuum variable capacitors capable of producing a total capacitance range of

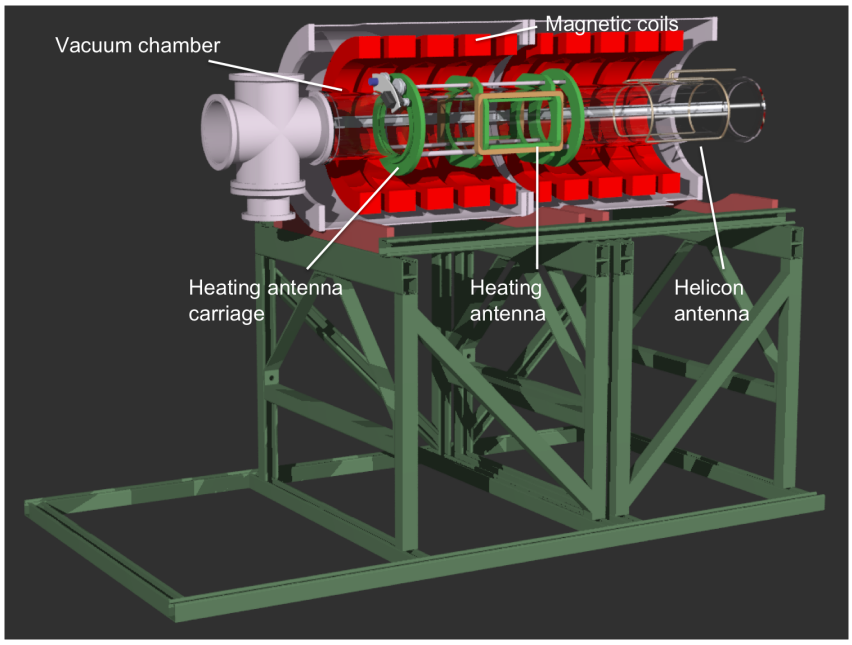

(a) Rendering of the experimental apparatus

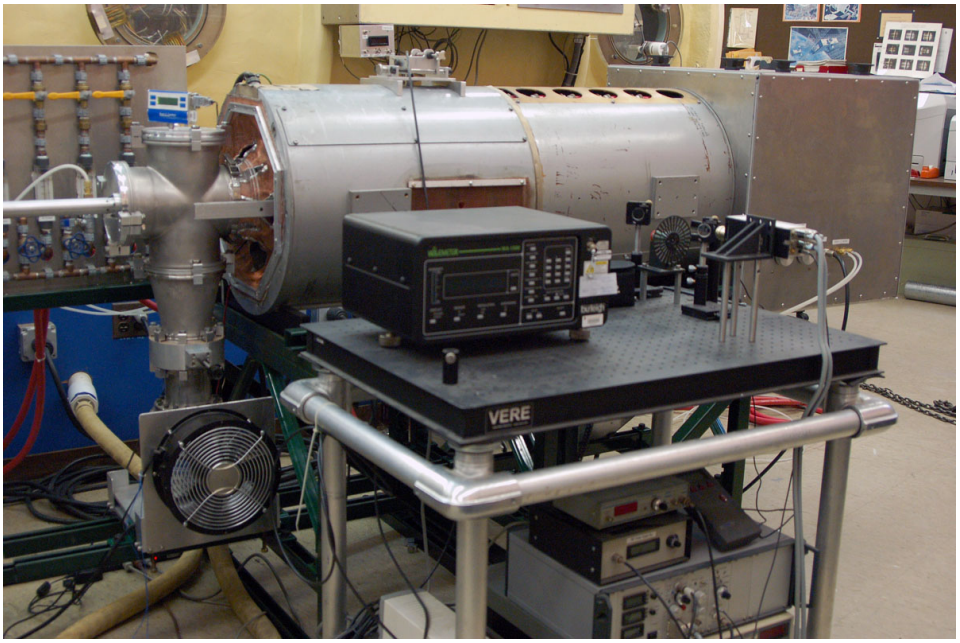

(b) Photograph of the experimental apparatus showing the LIF system in the foreground.

Figure 2. Schematic of the experimental apparatus.

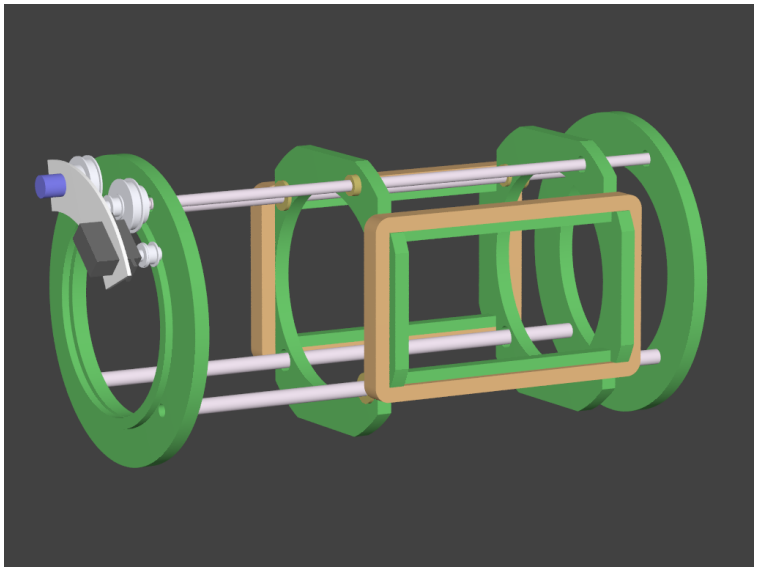

(a) Picture of heating antenna mounted on the vacuum vessel

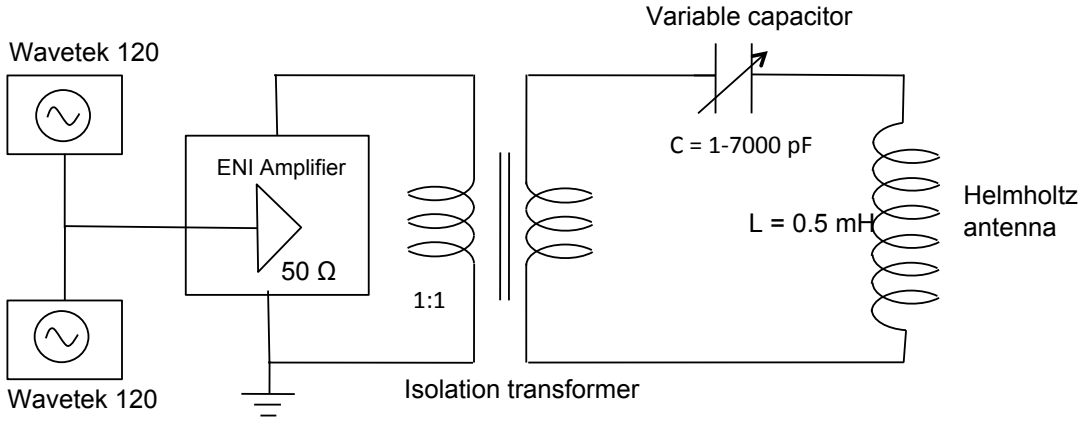

(b) Equivalent circuit diagram of Helmhotlz antenna with matching network and power amplifier.

Figure 3.

1-7000 pF. This setup, when connected in series with the heating antenna (L = 0.5 mH), allows us to tune the effective impedance of the antenna to approximately 5-10 Ω and thus increase the current in the antenna to the maximum 2.25 A output of the 100 W, 50 Ω amplifier.

D. Diagnostics

We employ three major diagnostics in our experiment. An RF-compensated Langmuir probe provideds background density and electron temperature measurements. A low-frequency directional coupler allows us to determine the amount of power delivered to waves launched from the heating antenna. And finally, we measure the ion temperature perpendicular to the magnetic field (denoted T_i for this investigation) by means of a Laser Induced Fluorescence (LIF) system based on the $3d^4F_{7/2}-4p^4D^0_{5/2}$ transition at 668.6130 nm of the metastable state of ArII. All LIF ion temperature measurements subsequently reported in this investigation are for steady state where the antenna is either activated (heating) or off (background measurement).

IV. Electrostatic Waves

As reported in Ref. 13, this experimental setup uses electrostatic ion cyclotron waves (EICW) launched perpendicularly to the magnetic field. The experimental dispersion relation for the waves is shown in Figure 4 and described by the equation[11]

$$\omega^2 = \omega_{ci}^2 + k^2 \frac{T_e}{m}, \tag{6}$$

where k is the wavenumber and m is the mass of the ion species. In our case, $k_{||} \approx .01$ cm^{-1} which was the lengthscale of the experiment. This allowed us to approximate the waves as approximately perpendicularly propagating. The maximum amount of heating power we could achieve in this investigation was 30 W, which we maintained for all frequencies by using the tuning network described above.

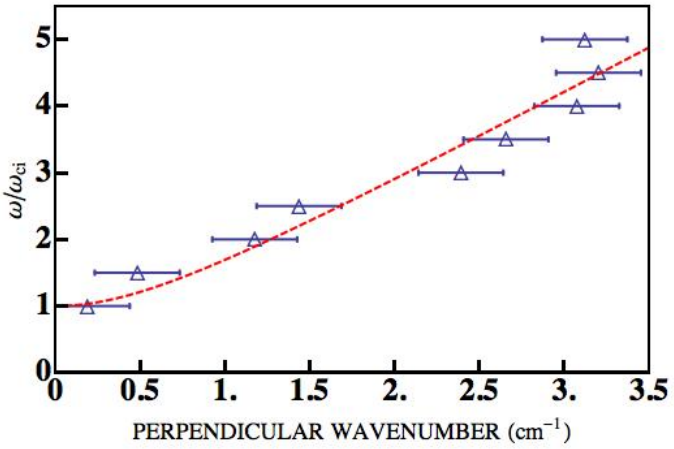

Figure 4. Empirically observed dispersion relation for electrostatic waves. The dotted line is a theoretical best fit using the EICW dispersion relation. The frequencies are normalized to the cyclotron frequency ω_{ci} that corresponds to a magnetic field of 500 G.

V. Frequency dependence of ion heating

In order to investigate ion heating in this setup, we first determined the background ion temperature to be 0.09 ± 0.03 eV through a series of LIF measurements. We next observed ion heating over several harmonics of the ion cyclotron frequency starting at the lower bound of our tuning range, $\nu = 2$. The total heating power in all cases and frequencies was 30 W, and the reported frequencies were accurate to 0.1 kHz.

The results of our heating measurements are shown in Figure 5. As can be seen, the SEW process exhibits heating levels well above the background temperature where the maximum value reported is approximately 0.23 eV. It is also evident that the heating improves significantly in the on-resonance cases where $\nu = n$ and n is an integer. Finally, we see qualitatively from the figure that SEW heating exhibits a maximum value at $\nu = 3$.

VI. Discussion

Before we can proceed in our comparison between our predictions and experimental data, we first must relate the normalized $\langle I_{eq} \rangle$ to the ion temperature. In particular, we see that since $\varepsilon \propto k$ and $\mu \propto k^2$, Eq. 3 implies that to second-order $T_i \propto \langle I_{eq} \rangle$ such that our expression for the normalized energy of the ensemble can be used as an indicator of ion temperature. With this in mind, we can immediately see from Figure 5 that one of our theoretical predictions has been verified. Namely, the heating improves markedly as we approach the on-resonance condition for the third, fourth, and fifth harmonics. The limitations on our frequency range prevented us from exploring additional harmonics, but the three observed peaks serve to corroborate our predictions.

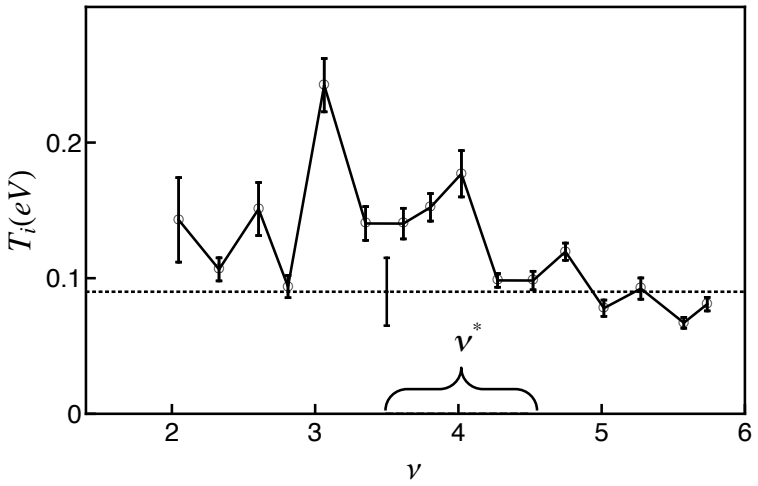

Figure 5. Frequency dependence of ion heating for SEW. The total heating power at each frequency is approximately 30 W. The cyclotron frequency is $f_{ci} = \omega_{ci}/2\pi = 19$ kHz, and the dotted line is the background ion temperature. The bracket denotes the analytically predicted range of optimal frequencies, ν^*, for the experimental parameters $T_i/T_e = 0.035$.

From our numerical results, we also see that there is an optimal frequency for heating. In order to compare this to our theoretical predictions, however, we recognize that the EICW has a dispersion relation where k can no longer be assumed, as done in Ref. 6, to be constant with frequency. In order to modify Eq. 3 and more precisely Eq. 4 to reflect this dependence, we express Eq. 6 in normalized coordinates as

$$\mu = \frac{T_{i0}}{T_e}\left(\nu^2 - 1\right). \tag{7}$$

where T_{i0} denotes the background ion temperature perpendicular to the magnetic field observed before heating. We substitute this expression into Eq. 4, but in keeping with the derivations of Ref. 6, we let $\mu \rightarrow \frac{T_{i0}}{T_e}\left(\|\nu\|^2 - 1\right)$. With this expression, we thus find that for our experimental parameters of $T_e = 3$ and $T_{i0} \approx 0.09$ eV, the range of frequencies that optimize $h(\nu)$ is given by $|\nu^*| = 4$. This range is shown in Figure 5 where we see our analytically derived value actually falls within one cyclotron harmonic from the experimentally measured value. This agreement lends support to our description of the physical processes at work in the SEW heating processes. The relatively small discrepancy between the predicted and experimental optimal frequencies may in part be due to the collisionless assumption for the derivations in Ref. 6. Additionally, as noted in Sec. II, on-resonance effects lead to a discrepancy in the numerical optimal frequency and the analytically predicted ν^*. This implies that these effects may also contribute to the difference between the observed experimental optimum and the $h(\nu)$ optimum, ν^*.

Regardless, it is apparent that the SEW process does exhibit an optimal frequency for heating and that our theoretical trends approximate this value. This lends support to our qualitative explanations summarized in brief in Sec. II and in more detail in Ref. 6 for this behavior. As an additional note, this experimental validation of our theoretical predictions lends additional credence to the other observations made in Ref. 6 work using the same analytical methods. Specifically, it is predicted that for sufficiently high wave amplitudes, the non-resonant beating electrostatic wave (BEW) heating should be optimizable *and* should outperform SEW heating. In order to investigate this possibility, future work will necessarily need to exceed the 30W heating power delivered in this experiment.

VII. Conclusion

In conclusion, we have provided the first experimental verification of our numerically and analytically predicted frequency dependence of SEW heating. Specifically, we showed that this heating exhibits marked improvement as we approach on-resonance and there exists a distinct optimal frequency for heating. This result should be particularly useful for future work that seeks to maximize the efficiency of this RF heating process, especially for plasma propulsion application, and it further serves as an encouraging guide for future

experimental investigations that explore additional electrostatic wave heating mechanisms, such as BEW heating.

VIII. Acknowledgements

The authors would like to express their gratitude to Mr. Robert Sorenson for his assistance with the design and implementation of the antenna impedance matching network. We would also like to thank Shuyue Guo for her work with the experimental setup calibration. This project was initially supported by the Air Force Office of Scientific Research. It is currently carried out with support from the National Science Foundation and the Program in Plasma Science Technology, Princeton Plasma Physics Laboratory.

References

[1]Cairns, R., *Radiofrequency heating of plasmas*, A. Hilger, 1991.

[2]Karney, C. and Bers, A., "Stochastic Ion Heating by a Perpendicularly Propagating Electrostatic Wave," *Physical Review Letters*, Vol. 39, No. 9, 1977, pp. 550.

[3]Karney, C., "Stochastic ion heating by a lower hybrid wave," *Physics of Fluids*, Vol. 21, No. 9, Sept. 1978, pp. 1584–1599.

[4]Porkolab, M., *Wave Heating and Current Drive in Plasmas*, edited by V. Granatsten and P. Colestock, New York: Gordon and Breach, 1985.

[5]Fisch, N., "Theory of current drive in plasmas," *Review of modern physics*, Vol. 59, No. 1, 1987, pp. 175–234.

[6]Jorns, B. and Choueiri, E. Y., "Ion Heating with Beating Electrostatic Waves," *Submitted for publication, June 15, 2010*, 2010.

[7]Benisti, D., Ram, A. K., and Bers, A., "Ion dynamics in multiple electrostatic waves in a magnetized plasma. I. Coherent acceleration," *Physics of Plasmas*, Vol. 5, No. 9, 1998, pp. 3224–3232.

[8]Benisti, D., Ram, A. K., and Bers, A., "Ion dynamics in multiple electrostatic waves in a magnetized plasma. II. Enhancement of the acceleration," *Physics of Plasmas*, Vol. 5, No. 9, 1998, pp. 3233–3241.

[9]Spektor, R. and Choueiri, E., "Effects of Ion Collisions on Ion Acceleration by Beating Electrostatic Waves," *International Electric Propulsion Conference (IEPC), Toulouse, France March 17-21, 2003. IEPC-03-65*, 2003.

[10]Spektor, R. and Choueiri, E. Y., "Ion acceleration by beating electrostatic waves: Domain of allowed acceleration," *Physical Review E*, Vol. 69, No. 4, April 2004, pp. 046402.

[11]Stix, T. H., *Waves in Plasmas*, Springer, 1992.

[12]Jorns, B. and Choueiri, E., "Design of an Experiment to Optimize Plasma Energization by Beating Electrostatic Wave," *45th AIAA/ASME/SAE/ASEE Joint Propulsion Conference*, No. 5367, 2009.

[13]Jorns, B. and Choueiri, E., "Experiment for Plasma Energization with Beating Electrostatic Waves," *31st International Electric Propulsion Conference Proceedings*, No. 199, 2009.

[14]Kline, J. L., Scime, E. E., Keiter, P. A., Balkey, M. M., and Boivin, R. F., "Ion heating in the HELIX helicon plasma source," *Physics of Plasmas*, Vol. 6, No. 12, Dec. 1999, pp. 4767–4772.